Supplementary Information

MFO@BCZT- and metformin-integrated biomimetic hydrogel for magnetoelectric stimulation-induced neurogenesis and neuroprotection in synergistically promoting brain tissue repair

Yuyan Wang[1,†], Jialu Li[1,†], Chengheng Wu[1,2], Polina Chernozem[3], Danila Koptsev[3], Enhao Zhang[1], Dmitry Wagner[3,4], Evgeny Gerasimov[5], Xiaoyin Liu[6], Gleb Sukhorukov[7,8], Maria Surmeneva[3], Roman Surmenev[3], Jie Ding[1], Dan Wei[1], Jing Sun[1], Roman Chernozem[3,*], and Hongsong Fan[1,*]

[1] National Engineering Research Center for Biomaterials, College of Biomedical Engineering, Sichuan University, Chengdu, Sichuan 610064, China

[2] Institute of Regulatory Science for Medical Devices, Sichuan University, Chengdu, Sichuan 610065, China

[3] National Research Tomsk Polytechnic University, 634050, Tomsk, Russia

[4] National Research Tomsk State University, 634050, Tomsk, Russia

[5] Boreskov Institute of Catalysis, 630090, Novosibirsk, Russia

[6] Department of Neurosurgery, West China Hospital, West China Medical School, Sichuan University, Chengdu, Sichuan 610041, China

[7] Center for Bio- and Medical Technologies (CBMT), Moscow 121205, Russia

[8] Life Improvement by Future Technology Center LLC (LIFT), Moscow 121205, Russia

[†] These authors contributed equally to this work.

* Corresponding authors: romanchernozem@gmail.com (R. Chernozem), hsfan@scu.edu.cn (H. Fan)

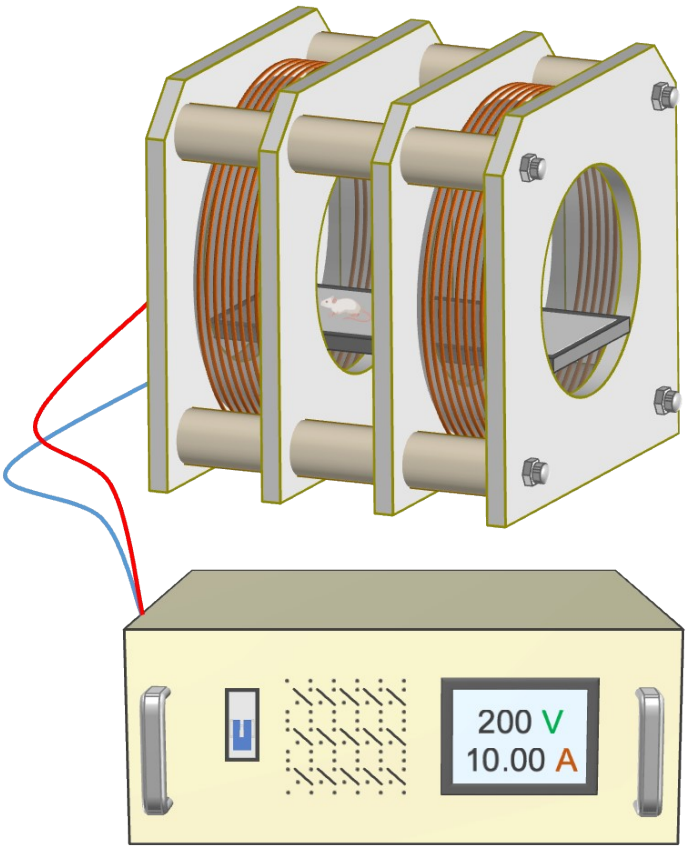

Fig. S1. Schematic illustration of the magnetic stimulation device.

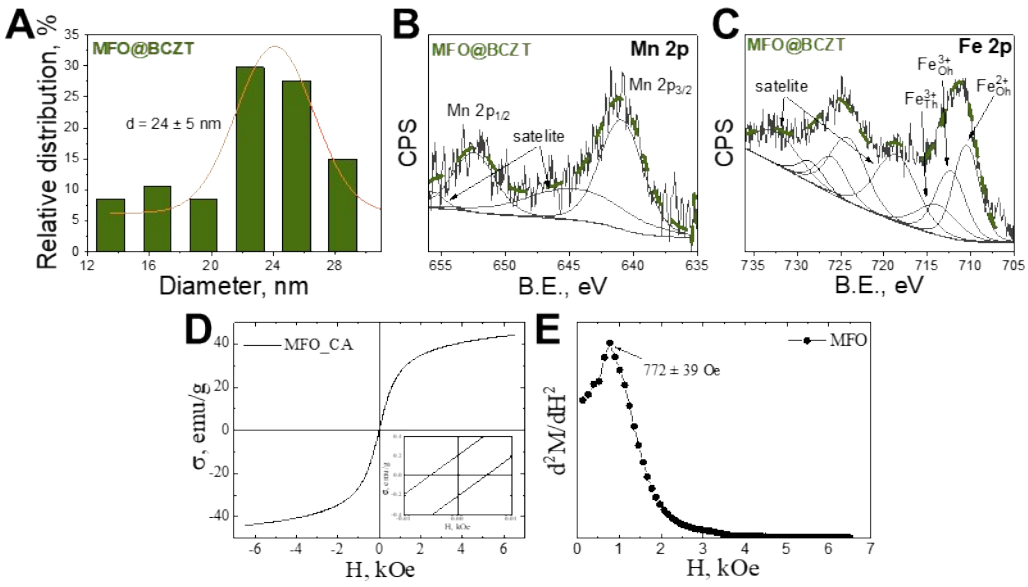

Fig. S2. (A) Relative distribution, High-resolution XPS spectra of (B) Mn 2p and (C) Fe 2p of MFO@BCZT NPs. (D) Magnetic hysteresis loop and (E) Second derivative of magnetization curve used for anisotropy field (H_a) determination of MFO cores.

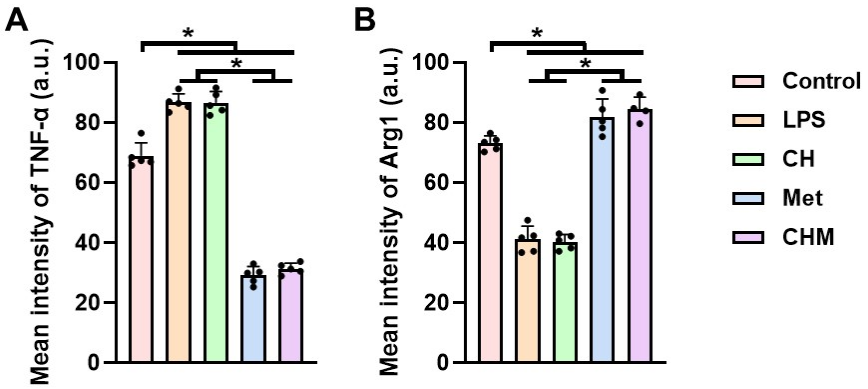

Fig. S3. Quantitative analysis of mean intensities of TNF-α (A) and Arg1 (B) based on the immunofluorescence staining images. n=5, *$p < 0.05$.

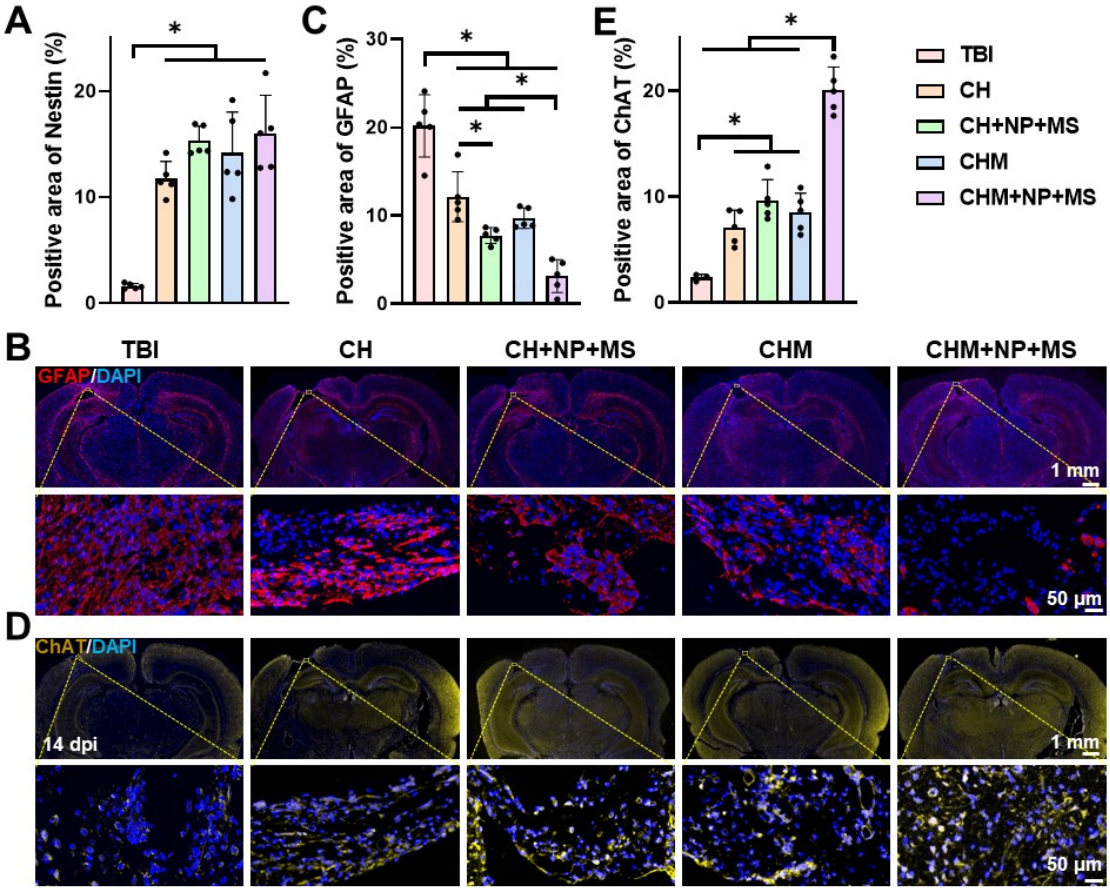

Fig. S4. (A) Quantitative analysis of the positive area of nestin according to corresponding immunofluorescence images. (B) Representative immunofluorescence images of GFAP-stained brain tissue sections. (C) Quantitative analysis of the positive area of GFAP according to corresponding immunofluorescence images. (D) Representative immunofluorescence images of ChAT-stained brain tissue sections. (E) Quantitative

analysis of the positive area of ChAT according to corresponding immunofluorescence images. n=5, *$p < 0.05$

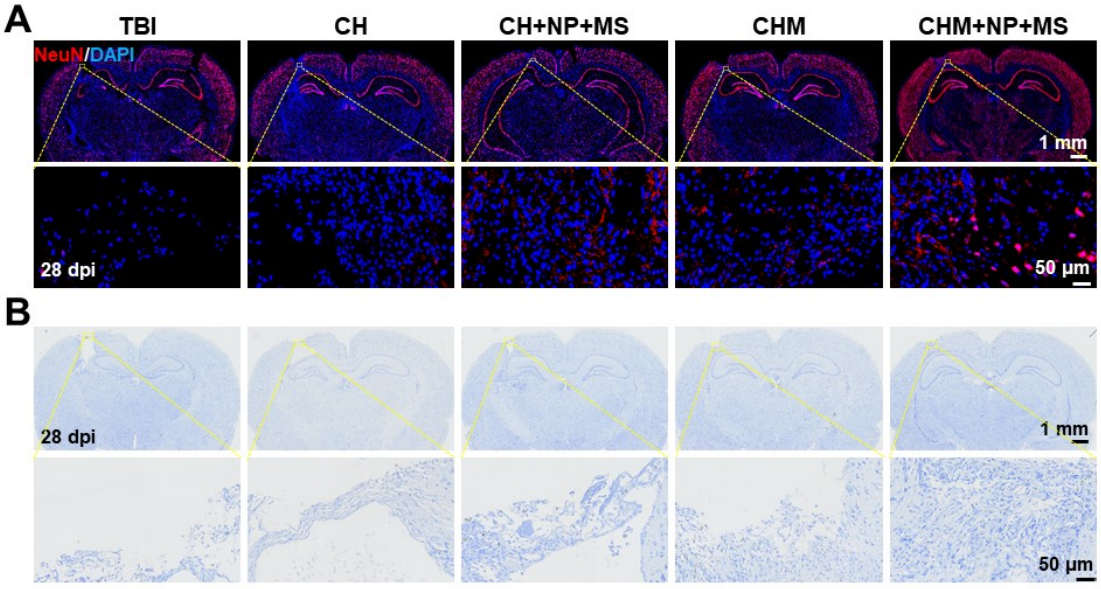

Fig. S5. (A) Representative immunofluorescence images of NeuN-stained brain tissue sections. (B) Typical Nissl staining images of brain tissue slices.

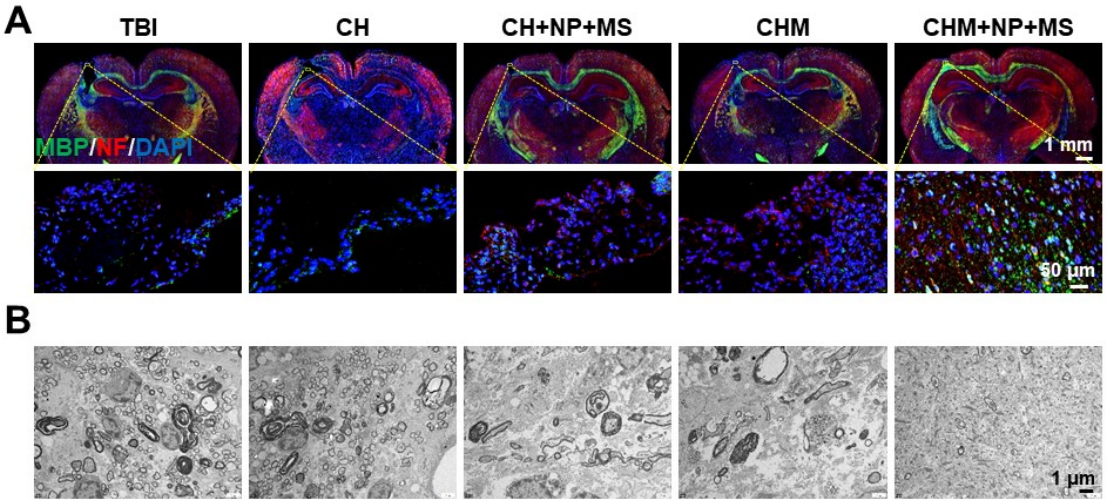

Fig. S6. (A) Representative immunofluorescence images of MBP (green)/NF (red)-stained brain tissue slices of all groups. (B) Representative TEM images showing the ultrastructure of myelin sheaths in lesions.

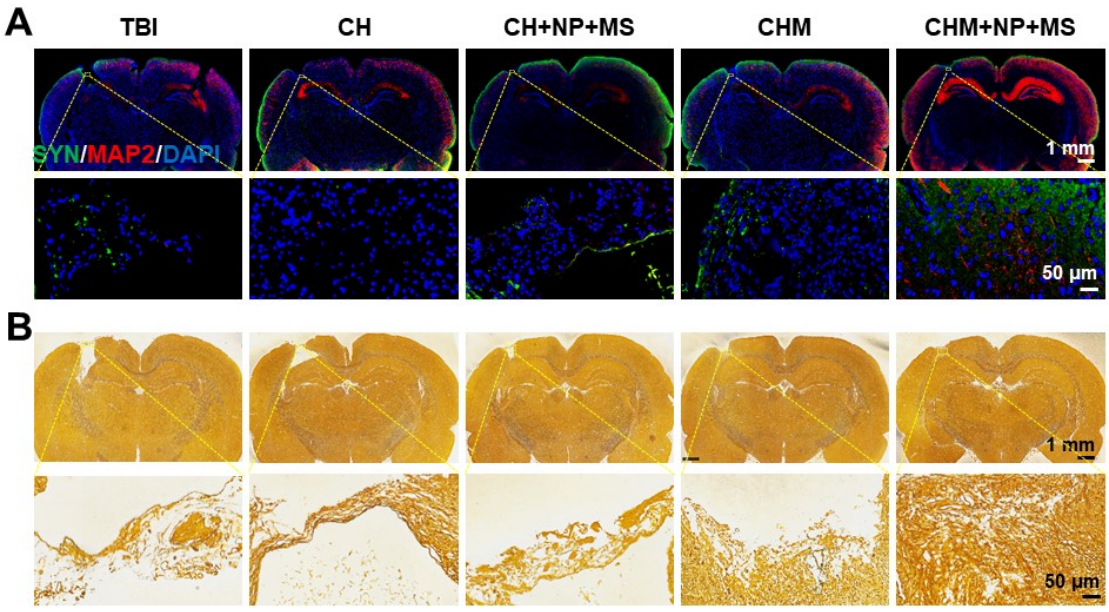

Fig. S7. (A) Representative immunofluorescence images of SYN (green)/MAP2 (red)-stained brain tissue slices of all groups. (B) Representative Bielschowsky silver staining images of brain tissue slices of all groups.

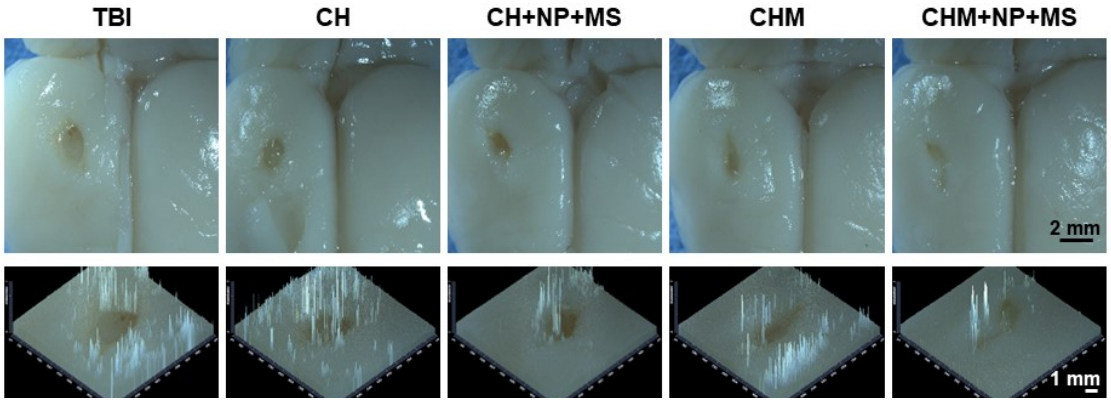

Fig. S8. Typical stereomicroscope images of brains in all groups.

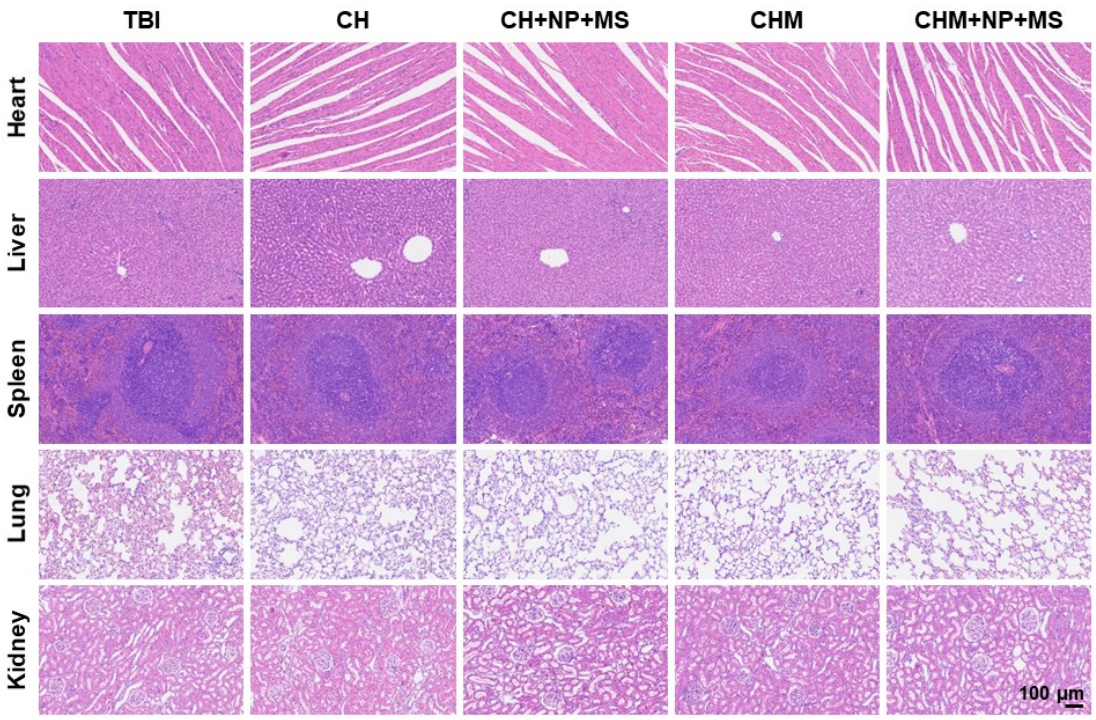

Fig. S9. Representative H&E staining images of the major organs of all groups.